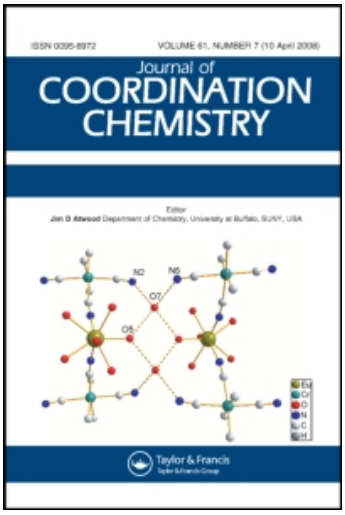

Journal of Coordination Chemistry
Publication details, including instructions for authors and subscription information:
http://www.informaworld.com/smpp/title~content=t713455674

Synthesis, spectral and theoretical studies on axial coordination of dinuclear Salen zinc(II) complexes

Jia-Mei Chen[a]; Wen-Juan Ran[a]; Feng Gao[a]; Ruan Duan[a]; Ying-Hui Zhang[a]; Zhi-Ang Zhu[a]
[a] Department of Chemistry, Nankai University, Tianjin, P.R., China

To cite this Article Chen, Jia-Mei , Ran, Wen-Juan , Gao, Feng , Duan, Ruan , Zhang, Ying-Hui and Zhu, Zhi-Ang(2007) 'Synthesis, spectral and theoretical studies on axial coordination of dinuclear Salen zinc(II) complexes', Journal of Coordination Chemistry, 60: 22, 2485 — 2497
To link to this Article: DOI: 10.1080/00958970701275782
URL: http://dx.doi.org/10.1080/00958970701275782

Journal of Coordination Chemistry
Vol. 60, No. 22, 15 November 2007, 2485–2497

Taylor & Francis
Taylor & Francis Group

Synthesis, spectral and theoretical studies on axial coordination of dinuclear Salen zinc(II) complexes

JIA-MEI CHEN, WEN-JUAN RAN*, FENG GAO, RUAN DUAN, YING-HUI ZHANG and ZHI-ANG ZHU

Department of Chemistry, Nankai University, Tianjin 300071, P.R. China

(*Received 2 February 2006; revised 5 August 2006; in final form 16 August 2006*)

Two dinuclear chiral Salen Zn(II) complexes Zn_2L (L = *N*,*N*′-(1*R*,2*R*)(−)-1,2-cyclohexylene-*bis*(3-hydroxybenzylideneimine)) and $Zn_2L'(OAc)_2$ (L′ = *N*,*N*′-(1*R*,2*R*)(−)-1,2-cyclohexylene-*bis*(3-methoxybenzylideneimine)) with compartmental, potentially hexadentate Schiff-base ligands L and L′ have been synthesized and characterized by elemental analyses, ^{1}H NMR, mass spectra, UV–Vis spectra and circular dichroism spectra. Their axial coordination with N-containing monodentate ligand (imidazole) and bidentate bridging ligands (ethylenediamine and 1,2-propylenediamine) have been studied by circular dichroism spectral titration, UV–Vis spectral titration and molecular modeling. The results of thermodynamic study, including standard association constants (K^{θ}), and thermodynamic parameters ($\Delta_r H_m^{\theta}$, $\Delta_r S_m^{\theta}$, $\Delta_r G_m^{\theta}$), together with the energy obtained from molecular modeling suggest that Zn_2L can bind two monodentate axial ligands or one bidentate ligand via a bridging mode with its two zinc atoms. However, the complex $Zn_2L'(OAc)_2$ can bind two bidentate ligands by a mode that each of its two zinc atoms coordinates to one of the two nitrogen atoms of the bidentate ligand. A small modification on the structure of a complex leads to a distinct binding mode with a certain ligand.

Keywords: Salen complexes; Axial coordination; Molecular modeling

1. Introduction

The chemistry of chiral Salen metal complexes has received increasing interest since they were first prepared and applied in epoxidation of unfunctionalized olefins in the early 1990s by Jacobsen [1] and Katsuki [2]. In the last two decades, many new chiral Salen complexes [3–6], including monomers, chain dimers and trimers, were designed and synthesized. Many of these complexes are good asymmetric catalysts for reactions such as aziridination [7], cyclopropanation [8, 9], epoxide ring opening [10, 11], hetero-Diels-Alder [12, 13] and sulfimidation [14, 15]. Axial coordination of metal complexes with a secondary ligand has been widely investigated in molecular recognition [16–20], molecular assembly [21, 22] and artificial metalloenzymes [23–25]. It has been reported

*Corresponding author. Fax: 86-22-23502458. Email: wjruan@nankai.edu.cn

Journal of Coordination Chemistry
ISSN 0095-8972 print/ISSN 1029-0389 online © 2007 Taylor & Francis
DOI: 10.1080/00958970701275782

that the presence of pyridine N-oxide derivatives has a significant effect on catalytic rates and total turnovers of the Salen metal catalysts [26]. The presence of organic bases such as DABCO, pyridine or triethylamine, has been found to give higher yields in chemical fixation of carbon dioxide catalyzed by a Salen Zn(II) complex [27]. Studies on axial coordination of Salen metal complexes with simple ligands can provide a basis for conceptualizing how Salen metal complexes might catalyze these kinds of reactions and for exploring how the properties of the Salen metal complexes might be utilized in developing novel catalysts. On the other hand, optimization of catalytic activities for a given process is typically achieved through methodically tailoring complexes. To get a fundamental knowledge of this subject and develop more structurally diverse catalysts, we have studied the axial coordination of several series of mononuclear Salen complexes [28–31], dinuclear Salen complexes bridged by a single aliphatic chain [32, 33] and trinuclear Salen complexes bridged by a crown ether [34]; many of these complexes showed interesting ligand binding properties.

In this report, starting from *bis*(salicylaldiminato) Schiff-base complexes, we design two chiral Salen ligands H_4L and H_2L' with N_2O_4 compartment by adding two O-donor atoms to the Salen structure. The N_2O_4 compartment incorporates two Zn(II) ions at adjacent positions to form chiral dinuclear Zn(II) complexes with only one Salen ligand. This type of complex can be expected to have novel and distinct axial coordination behavior. The two chiral Salen ligands H_4L and H_2L' derived from (*R*,*R*)-1,2-diaminocyclohexane and 2,3-dihydroxy-benzaldehyde or *o*-vanillin and their dinuclear chiral Salen Zn(II) complexes Zn_2L and $Zn_2L'(OAc)_2$ were synthesized and characterized. The axial coordination of the two complexes with monodentate imidazole and bidentate diamines was investigated in detail *via* circular dichroism and UV–Vis spectral titrations. Molecular modeling has been carried out to understand the axial coordination on a molecular level.

2. Experimental

2.1. *Materials and chemicals*

Chloroform ($CHCl_3$) was purified by standard methods [35], while other solvents were analytical grade, used as received. Zinc(II) acetate, 2,3-dihydroxy-benzaldehyde, *o*-vanillin and other reagents were commercial products used without further purification. (*R*,*R*)-1,2-diaminocyclohexane was prepared by a literature procedure [36].

2.2. *General procedures*

^{1}H NMR spectra were recorded on a Mercury Vx300 NMR spectrometer (300 MHz), using Me_4Si as internal standard. Elemental (C, H and N) analyses were carried out with a Perkin–Elmer 240C elemental analyzer. Electrospray mass spectra (ES-MS) were recorded on a Trace DSQ instrument. UV–Vis spectra were measured on a Shimadzu-265 spectrophotometer with a thermostated cell compartment. Circular dichroism spectra were recorded on a JASCO-715 spectropolarimeter.

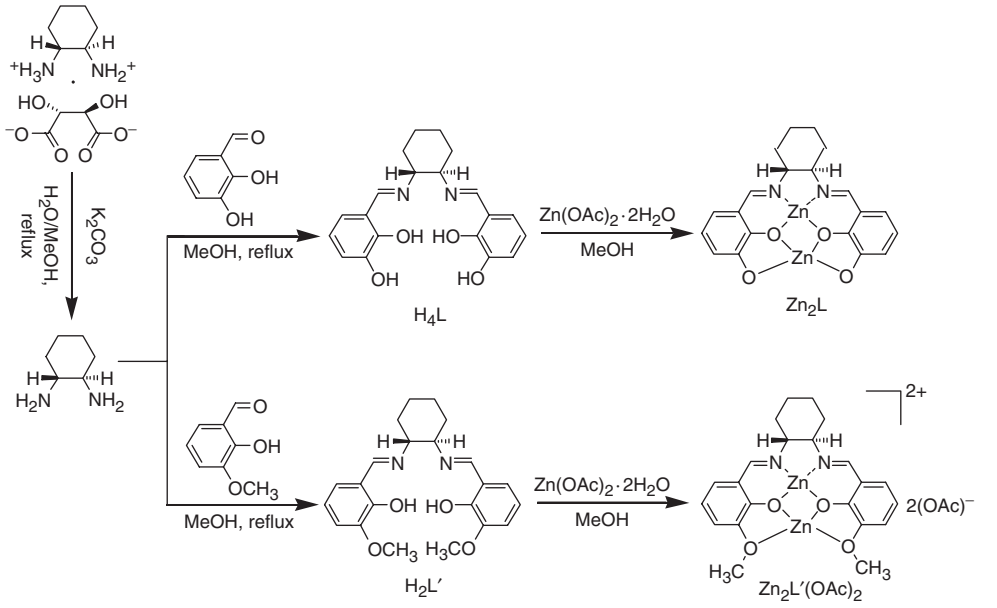

Scheme 1. Synthesis of Salen ligands H_4L, H_2L' and their dinuclear Zn(II) complexes.

2.3. *Synthesis and characterization*

The synthesis of chiral dinuclear Salen Zn(II) complexes is outlined in scheme 1.

2.3.1. H_4L. The ligand H_4L (*N*,*N*′-(1*R*,2*R*)(−)-1,2-cyclohexylene-*bis*(3-hydroxybenzylideneimine)) was prepared according to the literature method [37] with some modifications. To a solution of 276 mg (2 mmol) of 2,3-dihydroxy-benzaldehyde in 40 mL methanol, 114 mg (1 mmol) of (*R*,*R*)-1,2-diaminocyclohexane in 10 mL methanol was added dropwise. The resulting solution was refluxed for 4 h, cooled to room temperature and the solvent was removed. The orange solid was purified by silica gel column chromatography using diethyl ether/petroleum ether (2 : 1) as eluent and dried under vacuum.

Yield: 68.2%. Anal. Calcd for $C_{20}H_{22}N_2O_4$ (%): C, 67.78; H, 6.26; N, 7.90. Found: C, 67.54; H, 6.07; N, 8.11. ^{1}H NMR (d_6-DMSO) δ (ppm): 13.40 (s, 2H, OH), 8.90 (s, 2H, OH), 8.42 (s, 2H, N=CH), 6.78–6.74 (m, 2H, ArH), 6.75 (t, $J = 7.2$ Hz, 2H, ArH), 6.59 (t, $J = 6.9$ Hz, 2H, ArH), 3.40 (t, $J = 4.7$ Hz, 2H, chiral H), 1.91–1.45 (m, 8H, aliphatic H). UV–Vis ($CHCl_3$) data: λ_{max}/nm ($\log(\varepsilon/\text{mol}^{-1}\,\text{dm}^3\,\text{cm}^{-1})$): 262.2 (4.689), 307.4 (4.277), 431.4 (3.674). CD ($CHCl_3$) data: λ_{max}/nm ($\Delta\varepsilon/\text{mol}^{-1}\,\text{dm}^3\,\text{cm}^{-1}$): 270 (+5.853), 295 (−5.965).

2.3.2. Zn_2L. To a solution of 354 mg (1 mmol) of H_4L in 3 mL methanol, 440 mg (2 mmol) of zinc(II) acetate in 15 mL methanol was added in one portion, under stirring at room temperature for 2 h. The precipitated complex was collected by filtration. The resulting yellow solid was washed with methanol twice and dried under vacuum.

Yield: 85.6%. Anal. Calcd for $Zn_2C_{20}H_{18}N_2O_4 \cdot 2H_2O$ (%): C, 46.45; H, 4.29; N, 5.42. Found: C, 46.40; H, 4.24; N, 5.71. MS (ESI): $m/e = 480$ (M = 480). IR (KBr, cm^{-1}): ν_{OH} 3425, ν_{CH2} 2860, $\nu_{C=N}$ 1635 and $\nu_{C=C}$ 1456. UV–Vis ($CHCl_3$) data: λ_{max}/nm ($\log(\varepsilon/mol^{-1}\,dm^3\,cm^{-1})$): 240.8 (4.325), 283.8 (4.258), 376.6 (3.721). CD ($CHCl_3$) data: λ_{max}/nm ($\Delta\varepsilon/mol^{-1}\,dm^3\,cm^{-1}$): 276 (+4.569), 299 (−4.834), 338 (−4.052), 424 (−4.270).

2.3.3. H_2L'. To a solution of 304 mg (2 mmol) of *o*-vanillin in 30 mL methanol, 114 mg (1 mmol) of (*R*,*R*)-1,2-diaminocyclohexane in 10 mL methanol was added dropwise. The resulting solution was refluxed for 4 h, cooled to room temperature and the solvent was removed. The yellow microcrystalline product was purified by silica gel column chromatography using diethyl ether/petroleum ether (1 : 3) as an eluent, and dried under vacuum.

Yield: 76.8%. Anal. Calcd for $C_{22}H_{26}N_2O_4$ (%): C, 69.09; H, 6.85; N, 7.32. Found: C, 69.06; H, 6.83; N, 7.08. ^{1}H NMR (d_6-DMSO) δ (ppm): 13.51 (s, 2H, OH), 8.48 (s, 2H, N=CH), 6.98–6.91 (m, 4H, ArH), 6.74 (t, $J = 7.8$ Hz, 2H, ArH), 3.72 (s, 6H, OCH_3), 3.42 (t, $J = 4.4$ Hz, 2H, chiral H), 1.91–1.48 (m, 8H, aliphatic H). UV–Vis ($CHCl_3$) data: λ_{max}/nm($\log(\varepsilon/mol^{-1}\,dm^3\,cm^{-1})$): 240.6 (4.166), 261.4 (4.315), 332.8 (3.680). CD ($CHCl_3$) data: λ_{max}/nm ($\Delta\varepsilon/mol^{-1}\,dm^3\,cm^{-1}$): 254 (+5.063), 275 (−5.300), 333 (−4.785).

2.3.4. $Zn_2L'(OAc)_2$. To a solution of 378 mg (1 mmol) of H_2L' in 3 mL methanol, 440 mg (2 mmol) of zinc(II) acetate in 15 mL methanol was added in one portion and stirred at room temperature for 2 h. The precipitated complex was collected by filtration. The resulting pale yellow solid was washed with methanol twice and dried under vacuum.

Yield: 82.4%. Anal. Calcd for $Zn_2C_{26}H_{30}N_2O_8$ (%): C, 49.62; H, 4.80; N, 4.45. Found: C, 49.91; H, 4.78; N, 4.52. ^{1}H NMR ($CDCl_3$) δ (ppm): 8.26 (s, 2H, N=CH), 6.81 (d, $J = 8.1$ Hz, 4H, ArH), 6.62 (t, $J = 7.2$ Hz, 2H, ArH), 3.89 (s, 6H, OCH_3), 3.38 (s, 2H, chiral H), 2.91 (s, 6H, CH_3COO^-), 2.00 (s, 8H, aliphatic H). UV–Vis ($CHCl_3$) data: λ_{max}/nm ($\log(\varepsilon/mol^{-1}\,dm^3\,cm^{-1})$): 242.4 (4.422), 273.4 (4.317), 356.8 (3.851). CD ($CHCl_3$) data: λ_{max}/nm ($\Delta\varepsilon/mol^{-1}\,dm^3\,cm^{-1}$): 265 (+4.483), 286 (−4.858), 345 (+3.850), 378 (−4.454).

2.4. *Circular dichroism spectral titrations*

To a solution of 1.0×10^{-4} mol dm^{-3} of Zn_2L or $Zn_2L'(OAc)_2$ in $CHCl_3$ was added a solution of imidazole or diamines in $CHCl_3$. The solutions were allowed to incubate for 48 h before the spectra were recorded for equilibrium. Spectra in the range of 600–250 nm were recorded with [ligand]/[complex] ratios from 0 to 500 at room temperature.

2.5. *UV–Vis spectral titrations*

The thermodynamics experiments were performed with at least 100-fold excess of the axial ligands to the dinuclear complexes. Spectra titrations were carried out by following the changes on the π–π^* absorption bands of the zinc(II) complexes with increasing concentrations of the axial ligands at different temperatures (15, 20, 25,

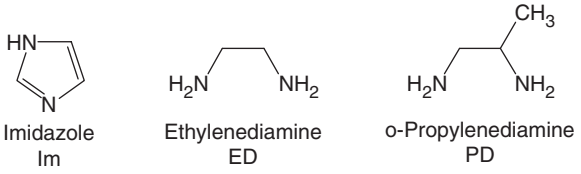

Scheme 2. Structrue of the axial ligands.

and 30°C). Generally, ten samples with a constant concentration (about 2.0×10^{-4} mol dm^{-3}) of the complexes were used with [ligand]/[complex] ratios from 0 to 3000. The solutions were allowed to incubate for 48 h before the spectra were recorded for equilibrium. The structures of the axial ligands are shown in scheme 2.

2.6. *Molecular modeling*

Molecular modeling was carried out with the Tripos force field in Sybyl 6.91 software (Tripos Inc.) on an SGI Indigo II workstation. Geometry optimization was performed with a gradient of 0.01 kcal mol^{-1}. Using the optimized conformation as initial conformation, simulated annealing was performed to obtain the minimal energy conformations of the dinuclear complexes, imidazole, diamines and their adducts.

3. Results and discussion

3.1. *CD spectral titration*

CD spectral changes of chiral dinuclear complexes, Zn_2L and $Zn_2L'(OAc)_2$, induced by the addition of imidazole or diamines are shown in figure 1. For Zn_2L–Im (imidazole) (figure 1a) and $Zn_2L'(OAc)_2$–PD (1,2-propylenediamine) (figure 1b), with the increasing concentration of the axial ligands, the Cotton effect peaks of the dinuclear complexes gradually reduced, while new Cotton effect peaks of their corresponding adducts gradually appear with considerable enhancement in intensity. The decrease in intensity shows loss of dinuclear complexes, with increase in the amount of the corresponding adducts in the solution. The isosbestic points observed indicate the complex–ligand systems are in a state of equilibrium. For Zn_2L and diamine systems (figure 1c, d), with the increasing concentration of diamines, the Cotton effect peaks of the dinuclear complexes do gradually reduce, but no new Cotton effect peaks arise, which indicates that their coordination modes probably differ with those above. Comparison of change in CD spectra of Zn_2L with the same concentration of ED (ethylenediamine) and PD is shown in figure 2, axial coordination capability of Zn_2L with ED is stronger than that with PD.

3.2. *UV–Vis spectrophotometric titration*

Interactions between the dinuclear complexes and the axial ligands (Im, ED and PD) at different temperatures were studied by UV–Vis spectroscopy. In solution, the reaction

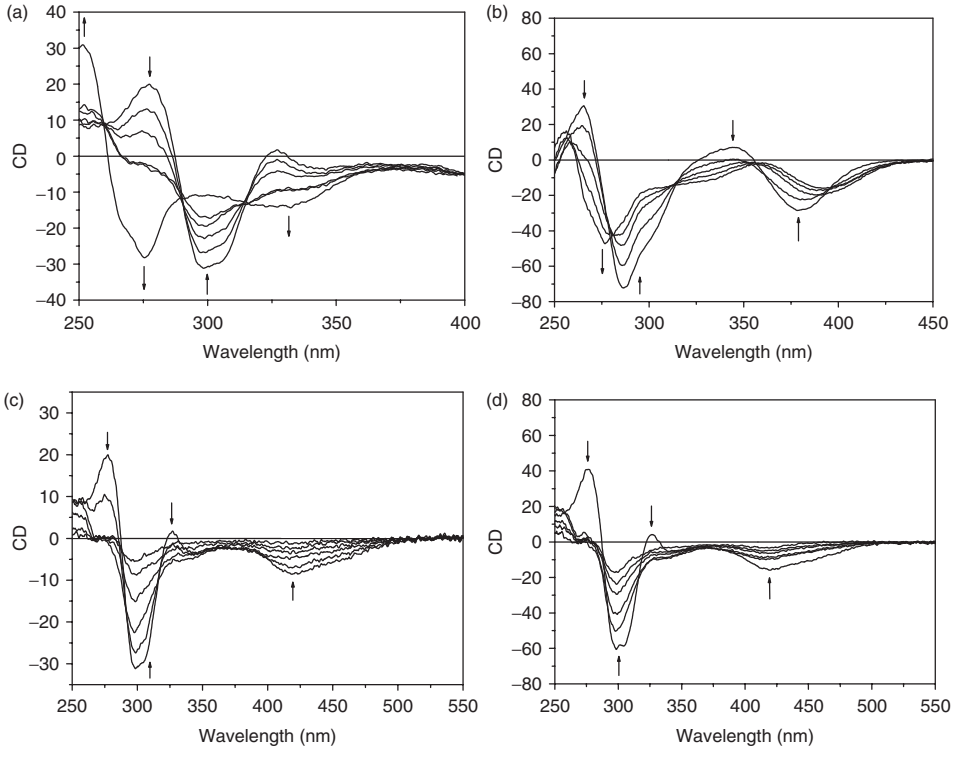

Figure 1. Changes in CD spectra of the dinuclear complexes with increasing concentrations of the axial ligands in $CHCl_3$ at 298 K: (a) $[Zn_2L] = 5.0 \times 10^{-5}$ mol dm^{-3}; [Im]/$[Zn_2L] = 0$–500; (b) $[Zn_2L'(OAc)_2] = 1.0 \times 10^{-4}$ mol dm^{-3}; [PD]/$[Zn_2L'(OAc)_2] = 0$–2; (c) $[Zn_2L] = 5.0 \times 10^{-5}$ mol dm^{-3}; [ED]/$[Zn_2L] = 0$–5; (d) $[Zn_2L] = 1.0 \times 10^{-4}$ mol dm^{-3}; [PD]/$[Zn_2L] = 0$–5.

between the dinuclear complexes and the axial ligands produces the desired adducts. By monitoring the changes in UV–Vis spectra, an increase in ligand concentration caused the formation of more adduct. A series of experiments was carried out with various axial ligands. The values of the association constants (K), at different temperatures were evaluated for the reaction represented as follows:

$$\text{Complex} + n\ \text{Ligand} \rightleftharpoons \text{Adduct}$$

$$K = \frac{[\text{Adduct}]}{[\text{Complex}][\text{Ligand}]^n} \tag{1}$$

where [Adduct], [Complex] and [Ligand] represent the equilibrium molar concentrations. The corresponding standard association constant, K^θ, is given by $K^\theta = K/(\text{mol dm}^{-3})^{-n}$.

A representative UV–Vis spectral titration of Zn_2L by the addition of imidazole is shown in figure 3(a). As the decrease of the bands at 390 nm and 285 nm (for Zn_2L) and the increase of the band at 250 nm (for Zn_2L–Im adduct), four isosbestic points are observed, showing a process of the consumption of Zn_2L and the production of the Zn_2L–Im adduct. Similar characteristics have also been observed in other complex–ligand systems.

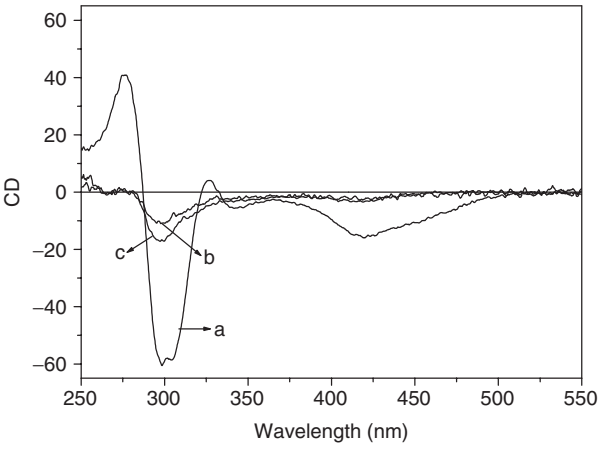

Figure 2. Comparison of changes in CD spectra of Zn_2L with the same concentration of diamine ligands: (a) Free Zn_2L, $[Zn_2L] = 1.0 \times 10^{-4}\,mol\,dm^{-3}$; (b) $[ED]/[Zn_2L] = 5$; (c) $[PD]/[Zn_2L] = 5$.

Since the thermodynamic experiments were carried out under the conditions with at least 100-fold excess of the ligand to the complex, the absorbance changes in the UV–Vis spectra can be analyzed by a linear fit according to equation (2) [38]:

$$\ln\left\{\frac{A_e - A_0}{A_\infty - A_e}\right\} = n \cdot \ln[L]_0 + \ln K^\theta \tag{2}$$

where A_e is the absorbance of solution at a certain wavelength at equilibrium, A_0 is the initial absorbance and A_∞ the final absorbance at the same wavelength, $[L]_0$ is the initial concentration of the axial ligand; n is a constant indicating the binding ratio of the ligands to the complexes in complex–ligand coordination systems. A plot of $\ln\{(A_e - A_0)/(A_\infty - A_e)\}$ *versus* $\ln[L]_0$ leads to a straight line with slope n and intercept $\ln K^\theta$. Figure 3(b) shows the fit to equation (2) of the Zn_2L–Im system at different temperatures.

As shown in table 1, the binding ratio of imidazole to Zn_2L is 2 : 1, while that of diamines to Zn_2L is 1 : 1. It is well known that planar mononuclear Zn(II) complexes can accept only one axial ligand [26, 27], so each zinc of dinuclear Zn_2L can bind one imidazole, and the binding ratio is 2 : 1. Similarly, Zn_2L binds to one diamine with its two zinc atoms coordinating with the two nitrogen atoms of diamines. The binding ratio is 1 : 1. Surprisingly, the binding ratio of propylenediamine to $Zn_2L'(OAc)$ is 2 : 1, which is similar to that of imidazole to Zn_2L. It is possible that each acetate ion in $Zn_2L'(OAc)_2$ is substituted by one PD. However, UV–Vis spectral titrations generally provide necessary, but not sufficient, clues to support a binding mode. More clues of binding will be obtained in the molecular modeling section.

From table 1, it is obvious that the complex–ligand interactions with both monodentate and bidentate N-donors are considerably weakened at higher temperatures, implying that their adducts are less stable than the dinuclear complexes themselves. For Zn_2L with diamine systems, the standard association constants decrease in an order $K^\theta(ED) > K^\theta(PD)$. The standard association constants are determined by both steric bulk and electronic effect of the methyl of PD, which can be seen more clearly in the molecular modeling section. For Zn_2L–Im and

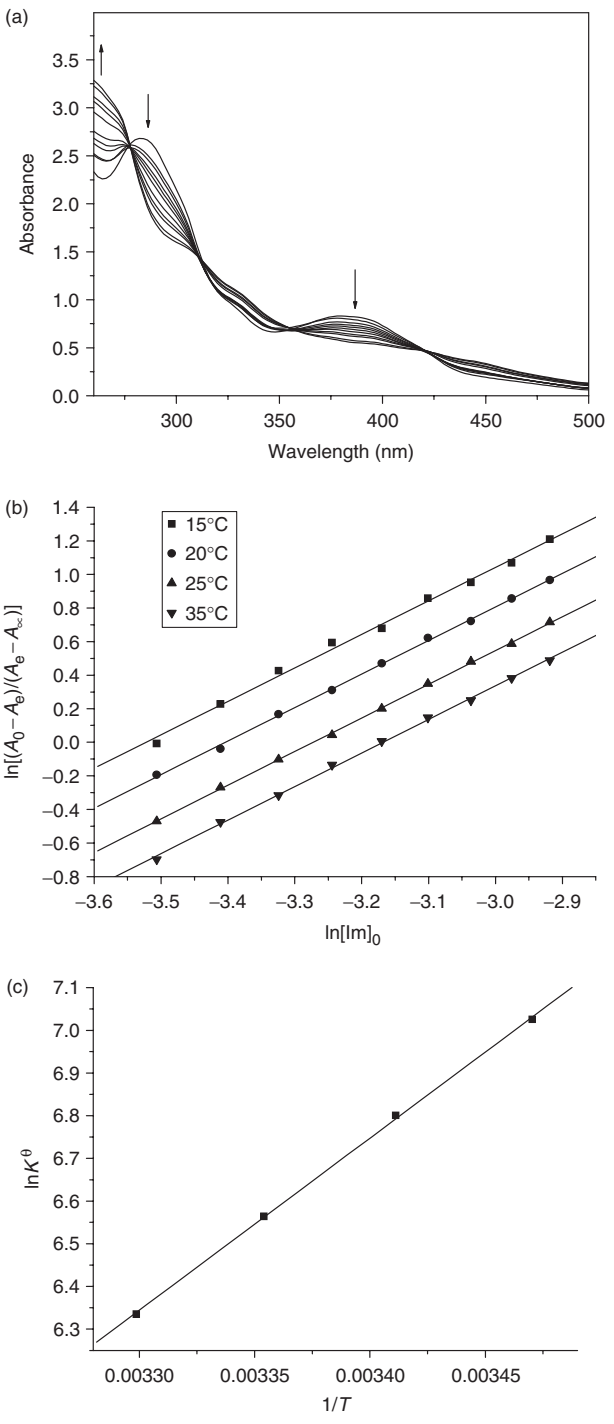

Figure 3. (a) UV–Vis spectral titration of Zn_2L with increasing concentrations of imidazole in $CHCl_3$ at 25°C: $[Zn_2L] = 2.0 \times 10^{-4}$ mol dm^{-3}, $[Im]/[Zn_2L] = 0$–1000. (b) Fit of the spectrophotometric data at different temperatures to equation (2). (c) Van't Hoff plots for the adduct formation reaction of Zn_2L with imidazole in $CHCl_3$.

Table 1. Standard association constants (K^{θ}) for the complex–ligand adduct formation reactions.

Complex	Ligand	K^{θ} 15°C	20°C	25°C	30°C	n
Zn_2L	Im	$(1.1 \pm 0.4) \times 10^3$	$(9.0 \pm 0.1) \times 10^2$	$(7.1 \pm 0.2) \times 10^2$	$(5.6 \pm 0.1) \times 10^2$	2.0
Zn_2L	ED	$(2.4 \pm 0.1) \times 10^1$	$(2.1 \pm 0.7) \times 10^1$	$(2.0 \pm 0.5) \times 10^1$	$(1.8 \pm 0.4) \times 10^1$	0.8
Zn_2L	PD	$(5.4 \pm 0.1) \times 10^0$	$(4.9 \pm 0.2) \times 10^0$	$(4.2 \pm 0.2) \times 10^0$	$(3.7 \pm 0.1) \times 10^0$	0.9
$Zn_2L'(OAc)_2$	PD	$(1.1 \pm 0.3) \times 10^4$	$(4.9 \pm 0.2) \times 10^3$	$(2.1 \pm 0.1) \times 10^3$	$(1.1 \pm 0.1) \times 10^3$	1.8

Table 2. $\Delta_r H^{\theta}_m$, $\Delta_r S^{\theta}_m$, and $\Delta_r G^{\theta}_m$ values for the complex–ligand adduct formation reactions.

Complex	Ligand	$-\Delta_r H^{\theta}_m$ (kJ mol^{-1})	$-\Delta_r S^{\theta}_m$ (J mol^{-1} K^{-1})	$-\Delta_r G^{\theta}_m$ (kJ mol^{-1})
Zn_2L	Im	33.6 ± 4.1	57.9 ± 9.8	16.4 ± 1.8
Zn_2L	ED	16.0 ± 2.1	15.4 ± 4.1	7.4 ± 0.9
Zn_2L	PD	18.5 ± 1.5	49.2 ± 2.2	3.8 ± 0.5
$Zn_2L'(OAc)_2$	PD	113.3 ± 1.7	315.8 ± 3.1	19.1 ± 0.3

$Zn_2L'(OAc)_2$–PD, the standard association constants are much higher, a result of the difference in coordination mode.

In order to have a better understanding of the thermodynamics of the adduct formation of the axial ligands with the complexes, it is important and helpful to consider the enthalpic and entropic contributions. The $\Delta_r H^{\theta}_m$ and $\Delta_r S^{\theta}_m$ values for the adduct formation reactions were calculated from the K^{θ} at four different temperatures according to the Van't Hoff equation (equation (3)):

$$\ln K^{\theta} = \frac{-\Delta_r H^{\theta}_m}{(RT)} + \frac{\Delta_r S^{\theta}_m}{R} \tag{3}$$

The enthalpy and entropy changes of adduct formation reactions were determined in the usual manner from the slopes and intercepts of the linear fit of $\ln K^{\theta}$ to $1/T$ (see in figure 3c). The Gibbs free energy changes, $\Delta_r G^{\theta}_m$, were calculated from equation (4):

$$\Delta_r G^{\theta}_m = \Delta_r H^{\theta}_m - T\Delta_r S^{\theta}_m \tag{4}$$

All the systems were treated by the same procedure and the results are summarized in table 2. Thermodynamic parameters $\Delta_r H^{\theta}_m$, $\Delta_r S^{\theta}_m$ and $\Delta_r G^{\theta}_m$ are all negative. Negative $\Delta_r H^{\theta}_m$ indicates that the complex–ligand systems give out thermal energy during the binding process. Meanwhile, the number of species changes to 1 from 2 or 3, therefore, $\Delta_r S^{\theta}_m$ are also negative values. These facts imply that the adducts formed in $CHCl_3$ solution are enthalpy stabilized but entropy destabilized. As a result, the negative value of $\Delta_r G^{\theta}_m$, determined by enthalpy and entropy, confirms the binding process is spontaneous.

3.3. *Molecular modeling*

The minimum energy conformation of the chiral dinuclear Salen Zn(II) complexes, the axial ligands (Im, ED and PD) and their corresponding adducts were obtained by the method of simulated annealing followed by a geometry optimization. Conformations of

the complexes and their corresponding adducts are shown in figures 4 and 5. The total energy (E_{total}) and its components of minimum energy conformation calculated by geometry optimization are shown in tables 3 and 4. The main components of energy are bond stretching, angle bending and electrostatic energy, indicating that formation of the

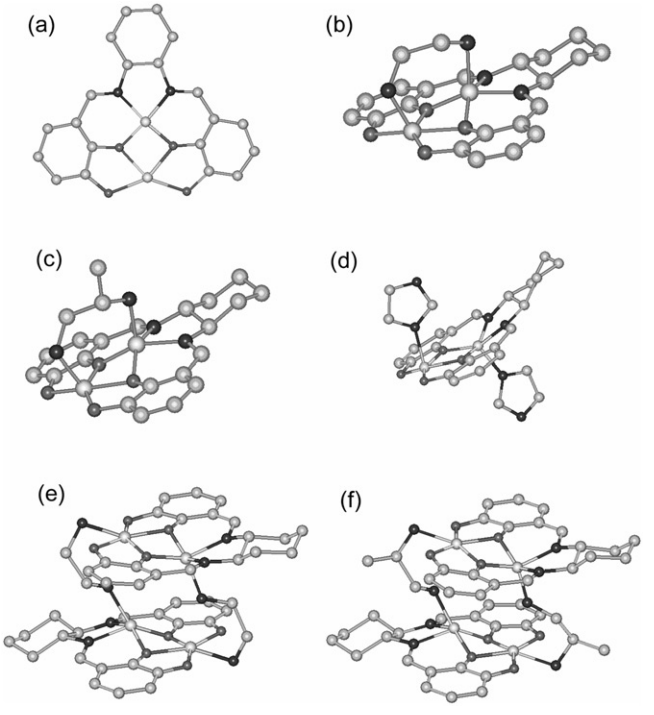

Figure 4. Minimal energy conformations of Zn_2L and its adducts: (a) Zn_2L, (b) $1Zn_2L$–1ED, (c) $1Zn_2L$–1PD, (d) $1Zn_2L$–2Im, (e) $2Zn_2L$–2ED, (f) $2Zn_2L$–2PD.

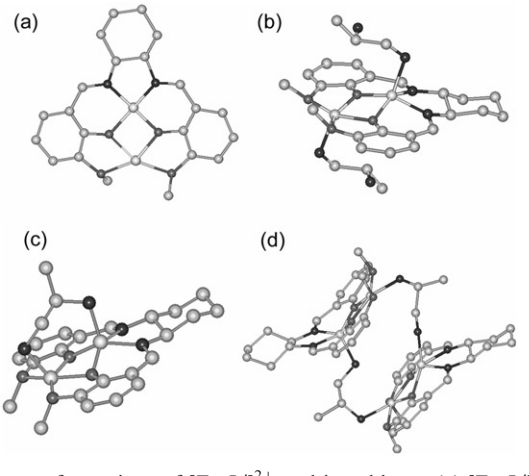

Figure 5. Minimal energy conformations of $[Zn_2L']^{2+}$ and its adducts: (a) $[Zn_2L']^{2+}$, (b) $1[Zn_2L']^{2+}$–2PD, (c) $1[Zn_2L']^{2+}$–1PD, (d) $2[Zn_2L']^{2+}$–2PD.

adducts is mainly determined by steric bulk and electronic effects. The adducts with lower total energy have better stability [39, 40].

As seen in figures 4(a) and 5(a), the minimal energy conformations of Zn_2L and $[Zn_2L']^{2+}$ are very close to the X-ray structure of similar Salen metal complexes [41–43], indicating that the molecular mechanics optimization and molecular dynamics simulation performed here are reliable. Zn_2L has a planar conformation with C_2 symmetry and coordinates with two imidazole molecules from both axial orientations simultaneously (figure 4d). For Zn_2L-diamine systems, according to the conclusion of UV–Vis spectra titration, the reaction of Zn_2L with diamines in $CHCl_3$ forms 1 : 1 adducts. Therefore, both diamines bridged complexes (figure 4b, c, 1 : 1 adducts) and dimer structures (figure 4e, f, 2 : 2 adducts) were sketched. From table 3, we can see that the total energy ascended in the order E_{total} (Zn_2L-1ED) $< E_{total}/2$ ($2Zn_2L$-2ED) and E_{total} (Zn_2L-1PD) $< E_{total}/2$ ($2Zn_2L$-2PD). These sequences imply that Zn_2L and diamine ligands form structures with bridging mode.

As seen in figure 5(a), two methyls of $[Zn_2L']^{2+}$ lie out of the Salen plane. Therefore, if $[Zn_2L']^{2+}$ binds PD via bridge mode (figure 5c) or dimerization (figure 5d), strong distortions of the Salen plane will occur. However, in the case of the 1 : 2 adduct of $[Zn_2L']^{2+}$–PD, as shown in figure 5(b), the flexibility of PD can efficiently avoid the spatial repulsion. Energies of 1 : 1 and 1 : 2 adducts of the $[Zn_2L']^{2+}$–PD system are summarized in table 4. The total energy ascends in the order E_{total} ($1[Zn_2L']^{2+}$-2PD) $< E_{total}$ ($1[Zn_2L']^{2+}$-1PD) $\ll E_{total}/2$ ($2[Zn_2L']^{2+}$-2PD), indicating that $[Zn_2L']^{2+}$ and ligand PD are apt to form 1 : 2 adducts.

For a stable coordination system, the energy gap ΔE ($\Delta E = E$ (adduct)–ΣE (complex)–ΣE (ligand)) is always a negative value. A bigger absolute value of ΔE

Table 3. Average energies (kcal mol^{-1}) of Zn_2L and its adducts.

Energy term	Zn_2L	$1Zn_2L$–2Im	$1Zn_2L$–1ED	$2Zn_2L$–2ED	$1Zn_2L$–1PD	$2Zn_2L$–2PD
Bond stretching energy	29.68	28.08	30.19	68.88	30.34	80.40
Angle bending energy	86.87	102.75	89.74	147.77	89.86	148.10
Torsional energy	5.65	6.47	8.04	17.83	8.07	18.25
Out of plane bending energy	0.94	0.94	0.85	4.49	0.84	3.97
1–4 van der Waal's energy	9.00	5.04	8.50	22.27	8.39	22.74
van der Waal's energy	−0.50	−5.45	−5.41	−3.36	−5.68	−2.78
1–4 Electrostatic energy	−3.02	−3.28	−17.13	18.76	−19.03	3.41
Electrostatic energy	89.68	123.83	100.78	244.58	101.89	242.76
Total energy	218.04	258.39	215.54	515.67	214.68	516.85

Table 4. Average energies (kcal mol^{-1}) of $[Zn_2L']^{2+}$ and its adducts.

Energy term	$[Zn_2L']^{2+}$	$1[Zn_2L']^{2+}$–2PD	$1[Zn_2L']^{2+}$–1PD	$2[Zn_2L']^{2+}$–2PD
Bond stretching energy	31.17	31.40	32.51	184.91
Angle bending energy	73.19	73.12	88.50	241.65
Torsional energy	9.38	10.25	11.70	63.59
Out of plane bending energy	0.90	0.92	0.96	42.66
1–4 van der Waal's energy	5.15	7.89	6.94	20.58
van der Waal's energy	−4.57	−15.74	−7.47	−14.31
1–4 Electrostatic energy	−20.43	−6.21	−16.92	34.82
Electrostatic energy	194.36	173.63	203.58	303.06
Total energy	289.15	275.25	319.82	876.96

Table 5. Energy gap (kcal mol^{-1}) between the free complexes, the free ligands and their corresponding adducts.

Adducts	$E_{Complex}$	E_{Ligand}	E_{Adduct}	ΔE*
1Zn_2L–2Im	218.04	24.812	258.39	−9.28
1Zn_2L–1ED		4.55	215.54	−7.05
2Zn_2L–2ED			515.67	70.49
1Zn_2L–1PD		3.42	214.68	−6.78
2Zn_2L–2PD			516.85	73.94
1$[Zn_2L']^{2+}$–2PD	289.15	3.42	275.25	−20.73
1$[Zn_2L']^{2+}$–1PD			319.82	27.25
2$[Zn_2L']^{2+}$–2PD			876.96	291.831

*$\Delta E = E_{Adduct} + a \times E_{Complex} + b \times E_{Ligand}$, a is stoichiometry of the salen complexes, b is stoichiometry of the axial ligands.

imply that formation of the corresponding adduct is more favorable. The values of ΔE in table 5 show that adducts of Zn_2L–Im (1 : 2) Zn_2L-ED (1 : 1, bridging mode), Zn_2L-PD (1 : 1, bridging mode), and $[Zn_2L']^{2+}$–PD (1 : 2) are stable. For Zn_2L and diamines systems, their stabilities vary in the order ED > PD. These results are in good agreement with the results of UV-Vis spectral titration.

4. Conclusions

The axial coordination of two new chiral dinuclear Salen zinc(II) complexes with monodentate and bidentate N-donor ligands have been investigated here. Spectral and molecular modeling studies suggest that Zn_2L can accept either two monodentate axial ligands or one bidentate axial ligand via the bridging mode. However, $Zn_2L'(OAc)_2$, with two additional methyls, binds two bidentate axial ligands. All the adducts are enthalpy stable but entropy unstable. Steric and electronic effects are important in formation of the adducts. Studies provide a basis for conceptualizing how Salen metal complexes efficiently catalyze diverse synthesis reactions with high selectivity and for exploring how the properties and the conformations of the Salen metal complexes might be utilized in the development of novel asymmetric catalysts.

Acknowledgements

This work was supported by a grant from the National Natural Science Foundation of China (Nos 20271030, 20303009).

References

[1] W. Zhang, J.L. Leoback, E.N. Jacobsen. *J. Am. Chem. Soc.*, **112**, 2801 (1990).
[2] R. Irie, K. Noda, Y. Ito, T. Katsuki. *Tetrahedron Lett.*, **31**, 7345 (1990).
[3] R. Konsler, J. Karl, E.N. Jacobsen. *J. Am. Chem. Soc.*, **120**, 10780 (1998).
[4] E.N. Jacobsen. *Acc. Chem. Res.*, **33**, 421 (2000).
[5] M.C. White, A.G. Doyle, E.N. Jacobsen. *J. Am. Chem. Soc.*, **123**, 7194 (2001).
[6] S.E. Denmark, E.N. Jacobsen. *Acc. Chem. Res.*, **33**, 324 (2000).
[7] S. Minakata, T. Ando, M. Nishimula, I. Ryu, M. Komatsu. *Int. Ed. Engl.*, **37**, 3392 (1998).

[8] T. Fukata, T. Katsuki. *Synlett*, 825 (1995).
[9] T. Uchida, B. Saha, T. Katsuki. *Tetrahed. Lett*., **42**, 2521 (2001).
[10] M. Tokunaga, J.F. Larrow, F. Kakiachi, E.N. Jacobsen. *Science*, **227**, 936 (1997).
[11] J.M. Ready. *J. Am. Chem. Soc*., **123**, 2687 (2001).
[12] S.E. Schans, J. Branalt, E.N. Jacobsen. *J. Org. Chem*., **63**, 403 (1998).
[13] K. Aikawa, R. Irie, T. Katsuki. *Tetrahed*., **57**, 845 (2001).
[14] C. Ohta, T. Katsuki. *Tetrahed. Lett*., **42**, 3885 (2001).
[15] M. Murakami, T. Uchida, T. Katsuki. *Tetrahed. Lett*., **42**, 7071 (2001).
[16] W.R. Scheidt, D.M. Chipman. *J. Am. Chem. Soc*., **108**, 1163 (1986).
[17] T. Mizutani, T. Ema, T. Tomita, Y. Kuroda, H. Ogoshi. *J. Am. Chem. Soc*., **116**, 4240 (1994).
[18] Y. Kuroda, Y. Kato, T. Higashioji, J. Hasegawa, S. Kawanawi, M. Takahashi, N. Shiraishi, K. Tanabe, H. Ogoshi. *J. Am. Chem. Soc*., **117**, 10950 (1995).
[19] T. Kurtan, N. Nesnas, Y.Q. Li, X.F. Huang, K. Nakanishi, N. Berova. *J. Am. Chem. Soc*., **123**, 5962 (2001).
[20] T. Kurtan, N. Nesnas, F.E. Koehn, Y.Q. Li, K. Nakanishi, N. Berova. *J. Am. Chem. Soc*., **123**, 5974 (2001).
[21] J.M. Lehn. *Supramolecular Chemistry Concepts and Perspectives*, VCH: Weinheim, Germany (1995).
[22] J.L. Atwood, J.E.D. Davies, D.D. MacNicol, F. Vögtle. *Comprehensive Supramolecular Chemistry*, Pergamon/Elsevier, Oxford (1996).
[23] X.X. Zhang, S.J. Lippard. *Inorg. Chem*., **39**, 4388 (2000).
[24] X.X. Zhang, P. Fuhrmann, S.J. Lippard. *J. Am. Chem. Soc*., **120**, 10260 (1998).
[25] R. Kachadourian, I. Batinic-Haberle, I. Fridovich. *Inorg. Chem*., **38**, 391 (1999).
[26] E.N. Jacobsen, L. Deng, Y. Furukawa, L.E. Martinez. *Tetrahed*., **50**, 4323 (1994).
[27] Y.M. Shen, W.L. Duan, M. Shi. *J. Org. Chem*., **68**, 1559 (2003).
[28] Y.L. Zhang, W.J. Ruan, X.J. Zhao, H.G. Wang, Z.A. Zhu. *Polyhedron*, **22**, 1535 (2003).
[29] W.J. Ruan, Y.L. Zhang, X.J. Zhao, D.Q. Jiang, Z.A. Zhu. *Chem. J. Chinese Universities*, **24**, 1657 (2003).
[30] W.J. Ruan, T. Liu, Y. Li, S.X. Luo, Z.A. Zhu. *Acta Chim. Sinica*, **61**, 1000 (2003).
[31] B.X. Zhu, W.J. Ruan, S.J. Wang, X.H. Cao, Z.A. Zhu. *Chinese J. Inorg. Chem*., **21**, 169 (2005).
[32] G.H. Hu, W.J. Ruan, F. Gao, Z.A. Zhu. *Acta Chim. Sinica*, **61**, 1969 (2003).
[33] B.X. Zhu, W.J. Ruan, F. Gao, X.H. Cao, Z.A. Zhu. *Chem. J. Chinese Universities*, **26**, 412 (2005).
[34] F. Gao, W.J. Ruan, J.M. Chen, Y.H. Zhang, Z.A. Zhu. *Spectrochim. Acta A*, **62A**, 886 (2005).
[35] D.D. Perrin, W.L. Armarego, D.R. Perrin. *Purification of Laboratory Chemicals*, 2nd Edn, Pergamon, Oxford (1982).
[36] E.N. Jacobsen, L. Deng, Y. Furukawa, L.E. Martinez. *Tetrahed*., **50**, 4323 (1994).
[37] A. Aguiari, E. Bullita, U. Casellato, P. Guerriero, S. Tamburini, P.A. Vigato. *Inorg. Chim. Acta*, **202**, 157 (1992).
[38] H.L. Anderson, C.A. Hunter, M.N. Meah, J.K.M. Sanders. *J. Am. Chem. Soc*., **112**, 5780 (1990).
[39] G.H. Olive, S. Olive. *Angew. Chem., Int. Ed. Eng*., **13**, 549 (1974).
[40] S. Kowalak, R.C. Weiss, K.J. Balkus. *Chem. Commun*., 57 (1991).
[41] P.G. Cozzi. *Angew. Chem. Int. Ed*., **42**, 2895 (2003).
[42] G.A. Morris, H. Zhou, C.L. Stern, S.T. Nguyen. *Inorg. Chem*., **40**, 3222 (2001).
[43] D. Cunningham, P. McArdle, M. Mitchell, N. Ni Chonchubhair, M. O'Gara, F. Franceschi, C. Floriani. *Inorg. Chem*., **39**, 1639 (2000).